Available online at www.sciencedirect.com

ScienceDirect

Tetrahedron

Tetrahedron 63 (2007) 11828–11837

# The stereodynamics of 3,5-bis(trifluoromethylsulfonyl)-1,3,5-oxadiazinane and 1,3,5-tris(trifluoromethylsulfonyl)-1,3,5-triazinane—an experimental and theoretical study

Bagrat A. Shainyan,[a,*] Igor A. Ushakov,[a] Vladimir I. Meshcheryakov,[a] Uwe Schilde,[b] Andreas Koch[b] and Erich Kleinpeter[b,*]

[a] *Irkutsk Institute of Chemistry, Siberian Division of Russian Academy of Sciences, 1 Favorsky Street, 664033 Irkutsk, Russia*
[b] *Chemisches Institut der Universität Potsdam, PO Box 69 15 53, D-14415 Potsdam, Germany*

Received 17 May 2007; revised 25 August 2007; accepted 20 September 2007
Available online 23 September 2007

**Abstract**—Multinuclear dynamic NMR spectroscopy of 3,5-bis(trifluoromethylsulfonyl)-1,3,5-oxadiazinane (**3**) revealed the existence of two conformers with differently oriented $CF_3$ groups with respect to the ring, and two dynamic processes: ring inversion and restricted rotation about the N–S bond. Two transition states connecting the two conformers and corresponding to clockwise and counterclockwise rotations about the N–S bond were found; the calculated activation barriers of about 12 kcal/mol are in excellent agreement with those measured experimentally for the related molecule 1,3,5-tris(trifluoromethylsulfonyl)-1,3,5-triazinane (**1**). X-ray analysis proved the existence of the symmetric isomer of **3**, which is the minor isomer in solutions but the only one in the crystal due to packing effects. The normal Perlin effect ($J_{CH_{ax}} < J_{CH_{eq}}$) was observed for 2(6)-$CH_2$ in **3**, whereas the reversed Perlin effect was found for the 4-$CH_2$ group in **3** as well as for all $CH_2$ groups in **1** both experimentally and theoretically. The latter effect in compounds **1**, **3**, and 1-(methylsulfonyl)-3,5-bis(trifluoromethylsulfonyl)-1,3,5-triazinane (**2**) can be considered as a genuine reverse Perlin effect since larger values of $^1J_{CH}$ are observed for longer C–H bonds.

## 1. Introduction

The conformational behavior of substituted cyclohexanes as well as heterocyclohexanes has been the subject of numerous studies.[1–3] The ring normally adopts the *chair* conformation unless specific intramolecular interactions stabilize the *twist* (Ref. 3b and references therein) or *boat* conformer.[3d,f] Substituents at the ring normally prefer the sterically favored equatorial over the more strained axial position,[1] although exceptions may exist provided that the 1,3-*syn* interactions with the axial substituent are attractive (like in thiane *S*-oxides)[4] or absent (like in 1,3-dialkyl-1,3-diazinanes and 1,3,5-trialkyl-1,3,5-triazinanes with one or two alkyls equatorial and one axial).[5–7] Recently the stereodynamic behavior of 1,3,5-tris(trifluoromethylsulfonyl)-1,3,5-triazinane **1** obtained by the reaction of trifluoromethanesulfonamide with formaldehyde[8] and that of 1-(methylsulfonyl)-3,5-bis(trifluoromethylsulfonyl)-1,3,5-triazinane **2** isolated from the three-component condensation of trifluoromethanesulfonamide, formaldehyde, and methanesulfonamide[9] (cf. Scheme 1) have been investigated by the use of $^1H$, $^{13}C$, and $^{19}F$ NMR low-temperature spectroscopy as well as quantum chemical calculations.[10,11] To the best of our knowledge, no other stereochemical studies have been performed on 1,3,5-triazinanes bearing electron withdrawing groups at the nitrogen atom(s). At the same time, the presence of strong acceptors, like the triflyl group,

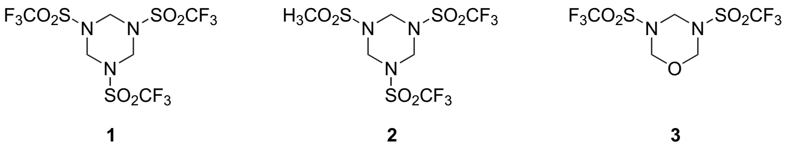

**Scheme 1**. Structure of compounds studied.

---

*Keywords*: *N*-Trifluoromethylsulfonyl derivatives of azinanes; Dynamic NMR; Perlin effect.

* Corresponding authors. Fax: +7 3952 419346; e-mail addresses: bagrat@irioch.irk.ru; kp@chem.uni-potsdam.de

0040–4020/$ - see front matter © 2007 Elsevier Ltd. All rights reserved.
doi:10.1016/j.tet.2007.09.041

may impart the nitrogen, to which it is attached, the properties of an $sp^2$ rather than $sp^3$-hybridized atom that, in turn, may result not only in specific stereochemical behavior, different from that for *N*-alkyl substituted analog, but also in interesting stereoelectronic effects in these heterocycles as was found to be the case for compound **2**.[11]

In this paper we report the stereochemical behavior of 3,5-bis(trifluoromethylsulfonyl)-1,3,5-oxadiazinane (**3** in Scheme 1), which was isolated from the product mixture formed upon condensation of trifluoromethanesulfonamide with formaldehyde.[8] The relative stability of possible conformers of **3**, $^1$H, $^{13}$C, and $^{19}$F dynamic NMR measurements, as well as the Perlin effect for the most stable conformer of **3** in solution are discussed. For the purpose of comparison, a detailed multinuclear NMR analysis of the related compound **1** (including the measurement of the Perlin effect) as well as its theoretical calculations was performed.

## 2. Results and discussion

### 2.1. 1,3,5-Tris(trifluoromethylsulfonyl)-1,3,5-triazinane 1

**2.1.1. $^1$H NMR, 2D{$^1$H–$^{13}$C}, and 2D{$^1$H–$^{15}$N} measurements.** For the mixture of conformers **1a**$\leftrightarrows$**1b** (Fig. 1), which were found to be the preferred conformers of 1,3,5-tris(trifluoromethylsulfonyl)-1,3,5-triazinane **1**,[10] the $^1$H NMR spectrum must contain two AB spin systems in the ratio of 1:2 belonging to 4-CH$_2$ and 2,6-CH$_2$ groups in **1a**, and one AB spin system of all CH$_2$ groups in **1b**.

The spectrum in acetone-$d_6$ at 223 K shows six doublets, which were grouped into three AB spin systems with regard to cross-peaks in the 2D{$^1$H–$^{13}$C} spectrum (Fig. 2a) and assigned considering their relative intensities and $^2J_{HH}$ coupling constants. The chemical shifts and the values of $^2J_{HH}$ and $^1J_{CH}$ are given in Table 1. The direct coupling constants $^1J_{CH}$ were obtained from cross-sections of the 2D heteronuclear {$^1$H–$^{13}$C} HSQC spectrum (Fig. 2b) recorded without wide band decoupling from $^{13}$C by GARP pulse sequence; the digital resolution for the proton channel in the HSQC experiments was 0.2 Hz. As can be seen from Table 1, for all CH$_2$ groups in conformers **1a** and **1b** a large reverse Perlin effect of 9–10 Hz is observed.

In the 2D{$^1$H–$^{15}$N} spectrum of **1** obtained at 223 K in the *hmbcgp* mode for $^2J_{NH}$ of 9 Hz, three $^{15}$N signals were observed and assigned according to cross-peaks with the corresponding axial protons. The signal at $\delta$ −283.3 ppm is coupled with H$_{ax}$ in **1b** and belongs to all nitrogen atoms in it, that at $\delta$ −285.0 ppm is coupled with 4-H$_{ax}$ in **1a** and belongs to N3 and N5, and the remaining signal at $\delta$ −282.5 ppm belongs to N1 in **1a**.

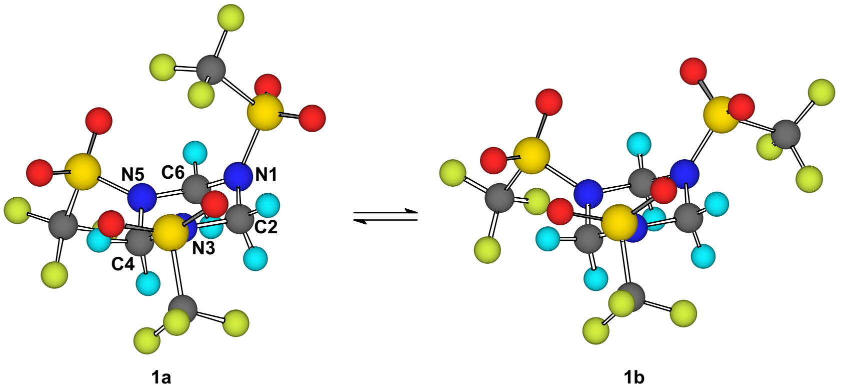

**Figure 1**. The '*inward*' (**1a**, $C_S$ symmetry) and '*outward*' (**1b**, $C_{3v}$ symmetry) rotamers of 1,3,5-tris(trifluoromethylsulfonyl)-1,3,5-triazinane.

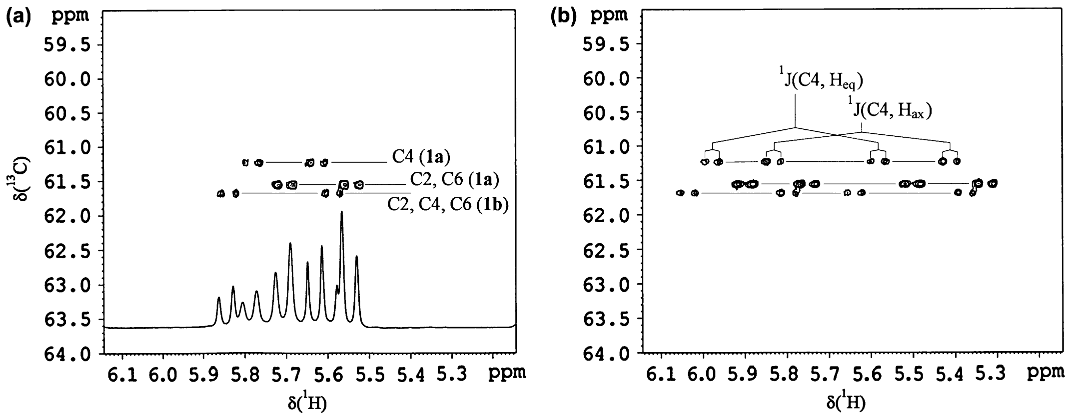

**Figure 2**. 2D{$^1$H–$^{13}$C} HSQC spectra of the mixture of rotamers **1a** and **1b** in acetone-$d_6$ at 193 K: (a) routine spectrum and (b) spectrum without wide band decoupling from $^{13}$C.

**Table 1**. Experimental (223 K, acetone-$d_6$) and calculated [GIAO/B3LYP/6-311+G(d,p)//B3LYP/6-311+G(d,p)] $^1$H chemical shifts ($\delta$/ppm) and $^1J_{CH}$ coupling constants (Hz) in conformers **1a** and **1b**

| Conformer | Group | Atom | Experimental | | | | Calculated | | |
|---|---|---|---|---|---|---|---|---|---|
| | | | $\delta_H$ | $^2J_{HH}$ | $^1J_{CH}$ | Perlin effect | $\delta_H$ | $^1J_{CH}$ | Perlin effect |
| **1a** | 2,6-CH$_2$ | H$_{ax}$ | 5.56 | 14.4 | 168.1 | −9.4 | 4.26 | 152.4 | −2.3 |
| | | H$_{eq}$ | 5.72 | | 158.7 | | 5.62 | 150.1 | |
| | 4-CH$_2$ | H$_{ax}$ | 5.64 | 13.4 | 169.4 | −9.8 | 4.26 | 151.5 | −2.9 |
| | | H$_{eq}$ | 5.80 | | 159.6 | | 5.48 | 148.6 | |
| **1b** | CH$_2$ | H$_{ax}$ | 5.60 | 13.7 | 168.4 | −9.3 | 4.38 | 153.0 | −4.5 |
| | | H$_{eq}$ | 5.85 | | 159.1 | | 5.70 | 148.5 | |

**2.1.2. Theoretical calculations.** B3LYP/6-311G(d,p) calculations of **1a** and **1b** performed in Ref. 10 showed the former to be more stable by 2.12 kcal/mol. The recalculated value of $\Delta E$ at the B3LYP/6-311+G(d,p) level is markedly lower, 1.44 kcal/mol. The lower stability of rotamer **1b** is consistent with its lower content (~20%) in the equilibrium mixture as measured in the $^1$H NMR spectrum at 223 K. Calculation of absolute shieldings and spin–spin coupling constants gave results which are in qualitative agreement with the experiment (Table 1). Calculated geometrical parameters and atomic charges for conformers **1a** and **1b** are presented in Table 2. The sum of the bond angles at nitrogen ($\sum_N$) is close to 360°, so the deviation of the nitrogen atom from planarity is insignificant. The axial C–H bonds are by 0.009–0.010 Å longer than the corresponding equatorial C–H bonds (Table 2) due to $n_N \rightarrow \sigma^*$(C–H$_{ax}$) and $n_N \rightarrow \sigma^*$(C–H$_{ax}$) interactions. Though the calculated values of the Perlin effect are notably smaller than the experimental ones, the essential result is that calculations correctly reproduce the sign of the Perlin effect (Table 1). It is noteworthy that *larger* values of $^1J_{CH}$ (Table 1) are observed for *longer* axial C–H bonds (Table 2).

**Table 2**. Elongation of axial bonds [$\Delta l = l$(C–H$_{ax}$)$-l$(C–H$_{eq}$)], Mulliken atomic charge differences ($\Delta q = q_{H_{eq}} - q_{H_{ax}}$), dihedral angles H$_{eq}$–C–N–S ($\theta$) and planarity of the nitrogen atom (sum of the bond angles, $\sum_N$) in molecules **1** and **3**

| Molecule | Position | $\Delta l$, Å | $\Delta q \times 10^3$ | $\theta$, deg | $\sum_N$, deg |
|---|---|---|---|---|---|
| **1a** | 2,6-CH$_2$ | 0.009 | 51 | 8.5 | 358.3 (N1) |
| | 4-CH$_2$ | 0.010 | 72 | 15.8 | 359.5 (N3, N5) |
| **1b** | All CH$_2$ | 0.009 | 57 | 0.6; 3.1 | 359.9 |
| **3a** | 2-CH$_2$ | 0.012 | 65 | 12.7 | 357.4 (N3) |
| | 4-CH$_2$ | 0.008 | 48 | 7.4; 0.4 | 359.0 (N5) |
| | 6-CH$_2$ | 0.013 | 50 | 2.6 | |
| **3b** | 2,6-CH$_2$ | 0.012 | 52 | 14.4 | 356.0 |
| | 4-CH$_2$ | 0.007 | 55 | 9.4 | |

## 2.2. 3,5-Bis(trifluoromethylsulfonyl)-1,3,5-oxadiazinane 3

**2.2.1. $^1$H NMR and 2D{$^1$H–$^{13}$C} measurements.** The $^1$H NMR spectrum of **3** in acetone-$d_6$ at 313 K shows two narrow singlets at $\delta$ 5.45 and 5.60 ppm in the 2:1 ratio belonging to the NCH$_2$O and NCH$_2$N methylene groups, respectively. Upon cooling, the signals become closer together and broaden, and below 243 K they start to decoalesce, becoming fully resolved below 203 K (Fig. 3a). The appearance of small doublets at $\delta$ 5.75 and 5.41 ppm (Fig. 3a), which belong to the minor conformer **3b** (Fig. 4) is also noted. The ratio of the two conformers, **3a**:**3b**, in acetone-$d_6$ is about 7:1. The remaining signals of **3b** and the corresponding $^1J_{CH}$ coupling constants were obtained from the 2D{$^1$H–$^{13}$C} NMR experiments. The assignment of the doublets at $\delta$ 5.39 and 5.51 ppm to the axial protons in the 2 and 6 positions of the ring was unequivocally proved by the presence of the corresponding cross-peak in the 2D NOESY spectrum of **3a** in acetone-$d_6$ at 193 K.

Similar dynamic behavior of the $^1$H NMR spectrum of **3** is observed in methanol-$d_4$. At 333 K sharp singlets of the NCH$_2$O and NCH$_2$N methylene groups are observed at $\delta$ 5.30 and 5.42 ppm, respectively. Upon cooling, they at first broaden and at 253 K merge, but below 233 K decoalescence begins and below 213 K the spectrum is fully resolved and 12 signals corresponding to six doublets of all nonequivalent axial and equatorial protons are clearly seen (Fig. 3b). The signals were grouped into three AB spin systems according to markedly different $J_{AB}$ values (Table 3) and with regard to cross-peaks in the 2D{$^1$H–$^{13}$C} spectrum (Fig. 5a). In the methanol-$d_4$ solution, the signals of the minor isomer **3b** are superimposed with those of the major isomer **3a**. The assignment was made as above, considering the relative intensities and $^2J_{HH}$ coupling constants. The measured values of the $^2J_{HH}$ coupling constants between the axial and equatorial protons were confirmed by the presence of the corresponding correlations in the 2D COSY spectrum. The values of $^1J_{CH}$ were obtained from cross-sections of 2D heteronuclear {$^1$H–$^{13}$C} HSQC spectrum (Fig. 5b) recorded using the same protocol as above for **1**. As can be seen from Table 3, $^1J_{CH_{ax}}$ is by 9–10 Hz larger than $^1J_{CH_{eq}}$ for NCH$_2$N in **3a** whereas for OCH$_2$N $^1J_{CH_{ax}}$ is slightly smaller than $^1J_{CH_{eq}}$.

As compared to compounds **1** and **2**, studied previously, compound **3** has only two bulky groups at the ring that should make the ring more flexible and result in lowering the temperature of decoalescence of signals in the NMR spectra. Indeed, the temperature of decoalescence for **3** (243 K) is notably lower than that for compounds **1** and **2** (263 K).[10,11]

**2.2.2. $^{13}$C NMR measurements.** At 293 K the $^{13}$C NMR spectrum of compound **3** in methanol-$d_4$ contains two singlets at 61.17 and 79.43 ppm corresponding to the NCN and NCO carbons, respectively. At 203 K the NCO signal decoalesces into two singlets at 79.25 ppm (major) and 79.61 (minor) corresponding to **3a** and **3b** conformers,

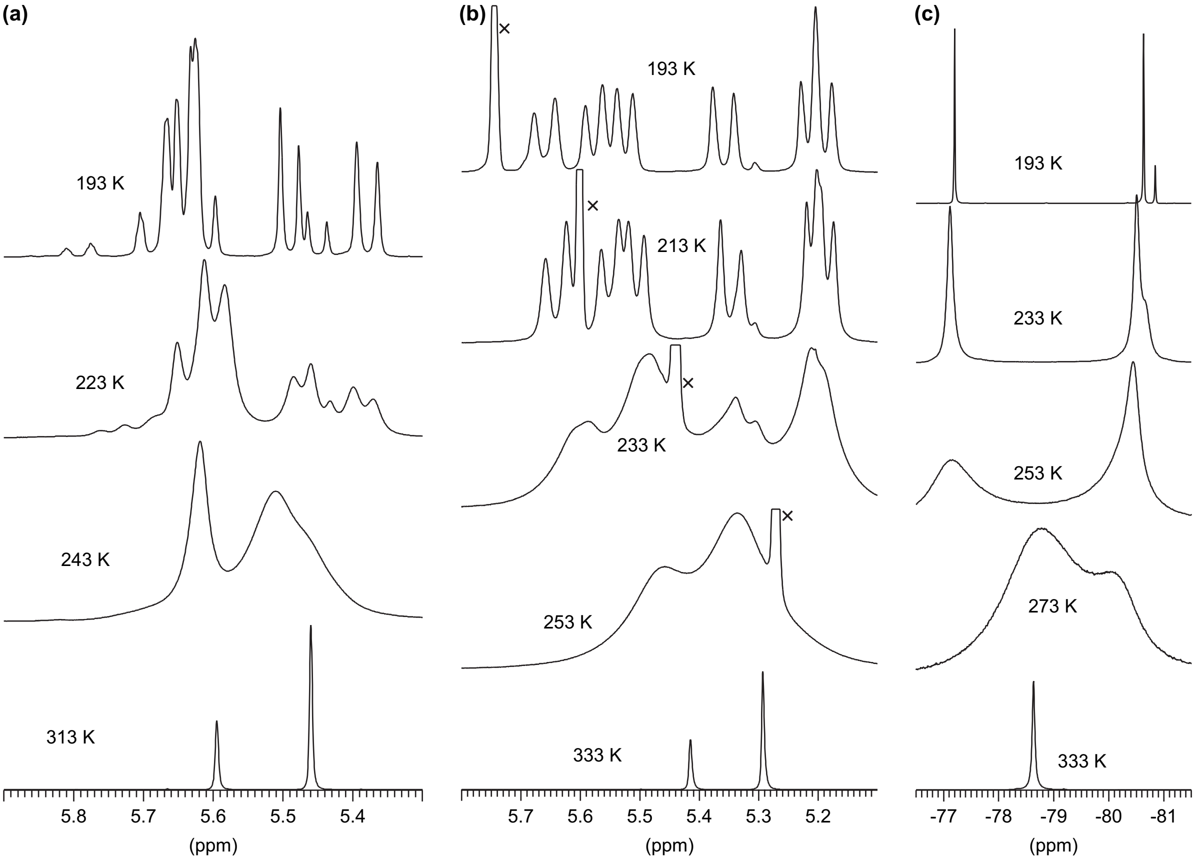

**Figure 3**. (a) $^{1}H$ NMR spectra of **3** in acetone-$d_6$; (b) $^{1}H$ NMR spectra of **3** in methanol-$d_4$ ('×' denotes the residual OH signal); (c) $^{19}F$ NMR spectra of **3** in methanol-$d_4$.

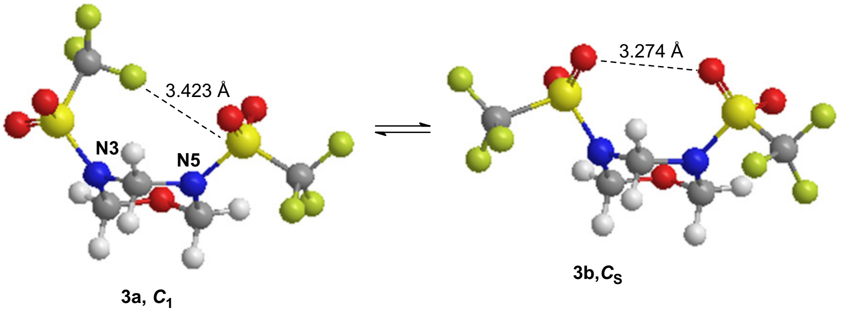

**Figure 4**. Equilibrium between the '*inward*' (**3a**, $C_1$ symmetry) and '*outward*' (**3b**, $C_S$ symmetry) rotamers of 3,5-bis(trifluoromethylsulfonyl)-1,3,5-oxadiazinane.

respectively. At 293 K the two $CF_3$ groups give an averaged quartet at 120.71 ppm ($J_{CF}$ 320.3 Hz), which at 203 K splits into two quartets at 120.39 ppm ($J_{CF}$ 318.9 Hz) and 120.70 ppm ($J_{CF}$ 321.6 Hz). The spectrum in acetone-$d_6$ is similar. The signals corresponding to the minor isomer **3b** were obtained from the 2D{$^{1}H$–$^{13}C$} spectrum. They are shifted by ca. 0.5 ppm downfield with respect to the corresponding signals of the major conformer **3a**.

**2.2.3. $^{19}F$ NMR measurements.** At 333 K both triflyl groups show one sharp singlet in the $^{19}F$ NMR spectrum of compound **3** in methanol-$d_4$ with $\delta_F$ −78.63 ppm. Below 273 K it starts to decoalesce to two singlets, which at 193 K resonate at $\delta_F$ −77.20 and −80.64 ppm, but the most remarkable is the emergence of a small singlet with $\delta_F$ −80.84 ppm at this temperature (Fig. 3c). The ratio of the signals is 1:1:0.23.

The observed nonequivalence of all protons in **3** confirms the structure of its major stereoisomer **3a** having two triflyl groups differently oriented with respect to the ring that is in compliance with the results of calculations. Direct evidence for the two different triflyl groups in **3a** is provided by the $^{13}C$ NMR spectrum showing two $CF_3$ quartets at low temperature. Judged from the analysis of the $^{13}C$ NMR spectra of **1** made in Ref. 10, where the assignment was facilitated by the different intensity of the signals, the upfield signal with smaller coupling constant $J_{CF}$ belongs

**Table 3**. Experimental (193 K, $CD_3OD$) and calculated [GIAO/B3LYP/6-311+G(d,p)//B3LYP/6-311+G(d,p)] $^1H$ and $^{19}F$ chemical shifts ($\delta$/ppm), and $^1J_{CH}$ and $^2J_{HH}$ coupling constants (Hz) in conformers **3a** and **3b**

| Group | Atom | Experimental | | | | Calculated | | | |
|---|---|---|---|---|---|---|---|---|---|
| | | $\delta_H$ or $\delta_F$ | $^2J_{HH}$ | $^1J_{CH}$ | Perlin effect | $\delta_H$ or $\delta_F$ | $^2J_{HH}$ | $^1J_{CH}$ | Perlin effect |
| $OCH_2N^3$ in **3a** | $H_{ax}$ | 5.15 (5.39) | 11.2 (11.7) | 165.5 (166.7) | 3.0 (2.3) | 4.72 | 11.3 | 151.0 | 9.0 |
| | $H_{eq}$ | 5.54 (5.66) | | 168.5 (169.0) | | 5.49 | | 160.0 | |
| $OCH_2N^5$ in **3a** | $H_{ax}$ | 5.18 (5.51) | 10.2 (10.8) | 166.0 (166.8) | 2.5 (2.2) | 4.73 | 9.8 | 151.9 | 7.5 |
| | $H_{eq}$ | 5.47 (5.66) | | 168.5 (169.0) | | 5.49 | | 159.4 | |
| $NCH_2N$ in **3a** | $H_{ax}$ | 5.32 (5.61) | 14.0 (14.4) | 167.5 (169.4) | −9.0 (−9.8) | 4.52 | 13.3 | 154.4 | −4.4 |
| | $H_{eq}$ | 5.62 (5.70) | | 158.5 (159.6) | | 5.65 | | 150.0 | |
| $OCH_2N$ in **3b** | $H_{ax}$ | (5.41) | (11.0) | (165.1) | (3.4) | 4.74 | 10.4 | 151.0 | 9.0 |
| | $H_{eq}$ | (5.60) | | (168.5) | | 5.50 | | 160.0 | |
| $NCH_2N$ in **3b** | $H_{ax}$ | (5.60) | (14.4) | (168.5) | (−10.3) | 4.62 | 12.8 | 154.9 | −5.5 |
| | $H_{eq}$ | (5.75) | | (158.2) | | 5.71 | | 149.4 | |
| $N^3SO_2CF_3$ | F | −77.20 | | | | −91.9 | | | |
| $N^5SO_2CF_3$ | F | −80.64 | | | | −98.3 | | | |
| $CF_3$ in **3b** | F | −80.84 | | | | −98.5 | | | |

Values in brackets refer to solution in acetone-$d_6$.

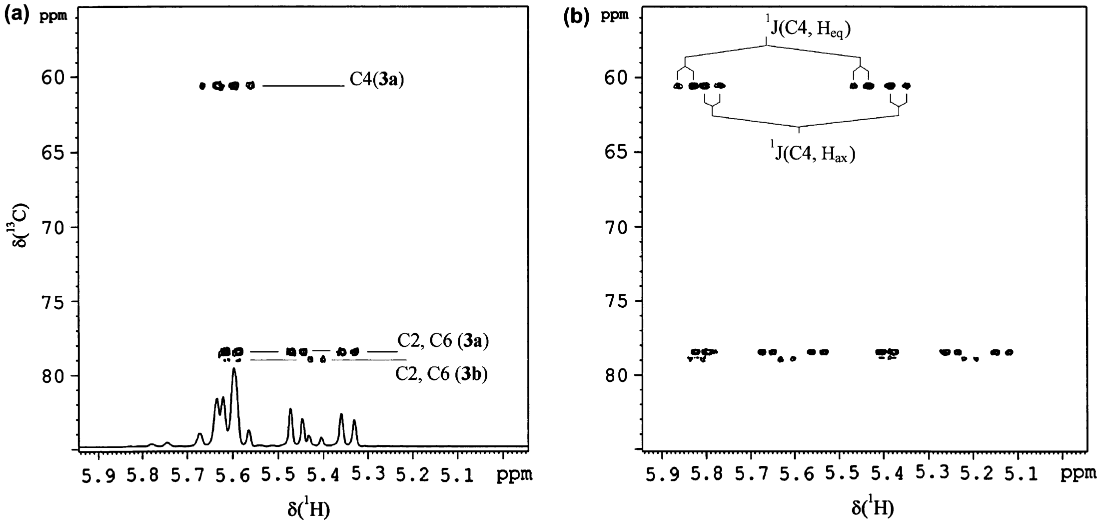

**Figure 5**. 2D{$^1H$–$^{13}C$} HSQC spectra of the mixture of rotamers **3a** and **3b** in acetone-$d_6$ at 193 K: (a) routine spectrum and (b) spectrum without wide band decoupling from $^{13}C$.

to the 'inward' $CF_3$ group and the downfield signal with larger $J_{CF}$ to the 'outward' one.

The low-temperature $^{19}F$ NMR spectrum of **3** not only corroborates these results but also provides direct evidence for the presence and the symmetry of the second rotamer, **3b**. The two $^{19}F$ signals of equal intensity belong to the 'inward' and 'outward' directed triflyl groups in **3a**, whereas the small upfield signal at $\delta_F$ −80.84 ppm belongs to two equivalent triflyl groups in **3b** (Fig. 3c). Closeness of the two upfield signals suggests that the signal at $\delta_F$ −80.64 ppm belongs to the 'outward' triflyl group in **3a** and that at $\delta_F$ −77.20 ppm to the 'inward' triflyl group. This is in accordance with the calculations, which show the fluorine atoms in the 'inward' triflyl group to be less shielded than in the 'outward' triflyl group. The $^{19}F$ NMR spectrum in Figure 3c is also in good quantitative compliance with the results of theoretical calculations. The energy difference of the two rotamers calculated from their experimental ratio of 8.7:1 at 193 K is 0.83 kcal/mol, which coincides excellently with the theoretically calculated $\Delta E$ value of 0.81 kcal/mol. The relative energies of the conformers are probably determined by stabilization of **3a** due to a reduced F···S contact (3.423 Å) and destabilization of **3b** due to a reduced O···O contact (3.274 Å) as depicted in Figure 5; for comparison, the same O···O distance in **3a** exceeds 4 Å.

**2.2.4. Theoretical calculations.** B3LYP/6-311+G(d,p) calculations of **3** revealed two conformational minima. The more stable conformer **3a** of $C_1$ symmetry has one triflyl group (attached to N3) directed inward with respect to the ring, whereas conformer **3b** of $C_S$ symmetry is 0.81 kcal/mol higher in energy and has both triflyl groups directed outward from the ring (Fig. 5). Chair-to-chair inversion of **3b** would make both $CF_3SO_2$ groups axial that is sterically impossible and allows to exclude the corresponding rotamer from consideration. The sum of the bond angles at nitrogen in the $CF_3SO_2N\langle$ fragment is 357.4° and 359° for the N3 and N5 atoms in **3a**, respectively, and 356° for both nitrogens in

**3b**, that is, all nitrogens have close to $sp^2$ hybridization (Table 2). The ring conformation in both **3a** and **3b** corresponds to virtually ideal *chair* conformer. Interconversion of conformers **3a** and **3b** may occur by clockwise (toward the C2 atom) or counterclockwise (toward the C4 atom) rotation about the N–S bond, that is, via the transition states $[\textbf{TS-1}]^{\ddagger}$ and $[\textbf{TS-2}]^{\ddagger}$, respectively (Fig. 6).

B3LYP/6-311+G(d,p) vibrational frequency calculations verified the existence of both transition states. $[\textbf{TS-1}]^{\ddagger}$ and $[\textbf{TS-2}]^{\ddagger}$ lie 11.67 and 12.66 kcal/mol higher than **3a** and have one imaginary frequency of −42 and $-46\ \text{cm}^{-1}$, respectively, corresponding mainly to rotation about the N–S bond and, thus, connecting conformers **3a** and **3b**. The lower calculated barrier $[\textbf{TS-1}]^{\ddagger}$ is in excellent agreement with the experimental value of 11.5 kcal/mol found for compound **3** from $T_c$=243 K, $\Delta\nu$=121 Hz and $J_{HH}$=14.1 Hz. The free energies of activation $\Delta G^{\neq}$ for the transition states $[\textbf{TS-1}]^{\ddagger}$ and $[\textbf{TS-2}]^{\ddagger}$ are 12.72 and 14.01 kcal/mol, respectively, that is, the contribution from the entropy term makes the free energy difference $\Delta\Delta G^{\neq}$ (1.29 kcal/mol), 0.3 kcal/mol larger than the enthalpy difference $\Delta\Delta H^{\neq}$ (0.99 kcal/mol) due to the more hindered and, hence, more 'tight' transition state $[\textbf{TS-2}]^{\ddagger}$.

**2.2.5. X-ray analysis.** The most remarkable result of the X-ray analysis of molecule **3** is that the less stable isomer **3b** is 'frozen' in the crystal. Apparently, this is the result of its higher symmetry leading to more dense packing of the molecules in the crystal. The molecule has $C_S$ symmetry, characterized by the presence of a mirror plane formed by atoms O1 and C4 with its two hydrogen atoms. The second half of the molecule is generated by mirroring. The calculated structure **3b** in Figure 5 perfectly matches the experimental one in Figure 7. For example, the calculated O···O distance of 3.274 Å almost coincides with the experimental value of 3.264 Å. The calculated sum of the bond angles at nitrogen in **3b** of 356° is also very close to the experimental one (357.7°). Table 4 summarizes the selected bond lengths and angles and torsion angles.

Experimental and calculated NMR parameters for conformers **3a** and **3b** are given in Table 3 and calculated geometrical parameters and atomic charges for both conformers are presented in Table 2. Similar to molecule **1**, the sum of the bond angles at nitrogen ($\sum_N$) is close to 360°. The axial C–H bonds are 0.010±0.0024 Å longer than the corresponding equatorial C–H bonds due to $n_X \rightarrow \sigma^*(C{-}H_{ax})$ and $n_Y \rightarrow \sigma^*(C{-}H_{ax})$ interactions (X=Y=N for 4-$CH_2$; X=N, Y=O for 2,6-$CH_2$). The calculations are in qualitative agreement with the experiment in that they correctly reproduce the sign of the Perlin effect (Table 3) in all cases.

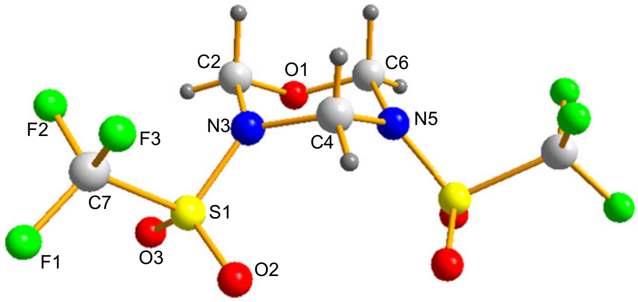

**Figure 7**. Single crystal X-ray structure of 3,5-bis(trifluoromethylsulfonyl)-1,3,5-oxadiazinane **3**.

**Table 4**. Selected bond lengths and angles and torsion angles for molecule **3b** (Fig. 7)

| Bond | Å | Bond angle | deg | Torsion angle | deg |
|---|---|---|---|---|---|
| O1–C2 | 1.414(4) | C2–O1–C6 | 109.9(3) | O1–C2–N3–C4 | 58.1(3) |
| C2–N3 | 1.459(3) | O1–C2–N3 | 109.1(2) | C2–N3–C4–N5 | −52.1(3) |
| N3–C4 | 1.459(3) | C2–N3–C4 | 112.9(2) | O1–C2–N3–S1 | −105.2(3) |
| N3–S1 | 1.599(2) | N3–C4–N5 | 108.2(2) | N5–C4–N3–S1 | 111.3(2) |
| S1–O2 | 1.415(3) | C2–N3–S1 | 122.33(19) | C2–N3–S1–C7 | −93.1(2) |
| S1–O3 | 1.412(2) | C4–N3–S1 | 122.55(18) | C4–N3–S1–C7 | 105.2(2) |

As to their absolute values, a general trend is that the calculated $\Delta J$ values for molecules **1**–**3** are less negative (Tables 1 and 3; see also Ref. 11) or more positive (Table 3) than the corresponding experimental $\Delta J$ values. Moreover, the difference between the experimental and calculated values of coupling constants $^1J_{CH}$ constitutes ca. 8–9 Hz for C–$H_{eq}$ and reaches even 14–16 Hz for C–$H_{ax}$ in molecules **1** and **3** (Tables 1 and 3). Very similar differences were obtained in Ref. 11 for compound **2** (the calculated values of $^1J_{CH}$ were not given). Most probably, this is due to the specific structure of molecules **1**–**3**, in particular, due to the presence of almost planar three-coordinated nitrogen atoms in the α-position to the methylene groups in the ring. Such an assumption is supported by the fact that at the same level of theory the experimental and calculated coupling constants $^1J_{CH}$ for various 4-silathiane *S*-oxides coincide within 1–2 Hz.[23] Some contribution may also come from a solvent effect since the experimental values of $^1J_{CH}$ in different solvents differ by up to 2 Hz (Table 3). However, the most

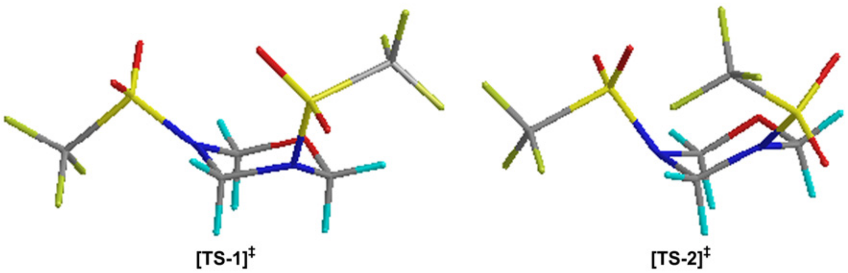
$[\textbf{TS-1}]^{\ddagger}$ $[\textbf{TS-2}]^{\ddagger}$

**Figure 6**. Transition states $[\textbf{TS-1}]^{\ddagger}$ and $[\textbf{TS-2}]^{\ddagger}$ for the **3a**→**3b** conversion corresponding to rotation of the '*inward*' directed $SO_2CF_3$ toward C2 or C4 atom in 3,5-bis(trifluoromethylsulfonyl)-1,3,5-oxadiazinane.

remarkable result is that *larger* values of $^1J_{CH}$ (Tables 1 and 3) are observed for *longer* axial C–H bonds (Table 2). Since in all cases the equatorial hydrogens are more positively charged (Table 2), the conclusion can be drawn that neither the length nor the polarity of the C–H bond is a factor determining the corresponding *$^1J_{CH}$ value and, hence, the sign of the Perlin effect*.

## 2.3. Perlin effect

Since 1969, when Perlin and Casu first showed that coupling constant $^1J_{CH}$ in β-D-glucose is 9 Hz smaller than that in α-D-glucose,[12] a number of works appeared concerning the problem of the anomeric effect and, in particular, its NMR manifestation, that is, the relationship between $J_{CH_{ax}}$ and $J_{CH_{eq}}$ in the anomeric position of the N-, O-, and S-containing six-membered heterocycles (see Ref. 13a for the list of relevant references available at that time). The stereoelectronic effect upon $^1J_{CH}$ has been called the 'Perlin effect' and originally it was interpreted in terms of hyperconjugation of the $n_X \rightarrow \sigma^*(C–H_{ax})$ type.[13] The 'normal' Perlin effect implies a smaller value of $J_{CH_{ax}}$ as compared to $J_{CH_{eq}}$ due to the above effect of the lone pair of a heteroatom. Experimentally, the involvement of the lone pair was proved by monotonic decrease of the value of $\Delta J = J_{CH_{eq}} - J_{CH_{ax}}$ for 4,6-dimethyl-1,3-dioxane, as the proton-donating ability of the solvent increased.[14] However, in the same work[14] the reverse Perlin effect ($J_{CH_{ax}} > J_{CH_{eq}}$) was found for $C^2$ in 4,6-dimethyl-1,3-dithiane and it was attributed by Wolfe et al. to $\sigma(C–S) \rightarrow \sigma^*(C–H_{eq})$ orbital interaction that outweighed the sulfur lone pair effect $n_S \rightarrow \sigma^*(C–H_{ax})$.[13] Since then, a number of papers have appeared related to experimental and theoretical analyses of the phenomenon.[3b,15–19]

For a long time the normal Perlin effect was associated with elongation and weakening of the C–$H_{ax}$ bond adjacent to a heteroatom X due to hyperconjugation $n_X \rightarrow \sigma^*(C–H_{ax})$. However, it is interesting to mention that while in 1990 Wolfe declared definitely that "*the shorter bond is characterized by the larger $^1J_{CH}$*",[13a] as soon as in 1994 Juaristi et al. showed that larger coupling constants may be associated with longer C–H bonds[15d] that allowed them to declare that there is "*no correlation between $^1J_{CH}$ constants and the corresponding C–H bond distances*".[15f] Moreover, the very concept of the $n_O \rightarrow \sigma^*(C–H_{ax})$ delocalization was questioned by Perrin et al. as primarily responsible for $^1J_{CH}$ (the Perlin effect)[20] and $^1J_{CC}$ coupling constants[21] in ethers. They showed that both constants continually decrease with the decrease of the dihedral angle HCOC or CCOC from 180° to 0°. Therefore, they suggested an electrostatic interaction between the oxygen atom lone pair dipole and that of the C–H or C–C bond to be the determining effect since it is this very effect that can result in monotonous decrease of $^1J_{CH}$ [20] and $^1J_{CC}$.[21] Yet, the authors specially emphasize that their conclusion is not necessarily general and do not exclude a contribution to $^1J_{CH}$ or $^1J_{CC}$ from $n_X \rightarrow \sigma^*(C–H_{ax})$ delocalization.[20,21] For example, such delocalization must be more pronounced for X=N since the nitrogen lone pair is of higher energy. Hyperconjugation effects on $^1J_{CH}$ were studied experimentally and theoretically by Tormena et al. who concluded that they are often intertwined with electrostatic effects in such a way that the two effects can either enhance or weaken each other.[22]

More entangled is the situation with the reverse Perlin effect. In addition to Bailey's finding of larger $J_{CH_{ax}}$ than $J_{CH_{eq}}$ for $C^2$ in 4,6-dimethyl-1,3-dithiane,[14] Juaristi et al. demonstrated that this is true for *all* $CH_2$ groups in 1,3-dithianes.[15b,d] Close to zero ($J_{CH_{ax}} \approx J_{CH_{eq}}$) or reverse ($J_{CH_{ax}} > J_{CH_{eq}}$) Perlin effects were also found for $C^2$ and $C^5$ in 1,3-oxathianes[15d] and for $C^5$ in 1,3-dioxanes,[15d,16a,b] 1,2,4-trioxanes,[16c] and 1,3-diazacyclohexanes.[16d] Comprehensive theoretical analyses of Juaristi[15f,g] and Alabugin[18] have shown that the values of $^1J_{CH}$ in heterocyclohexanes with heteroatom(s) X are governed by the balance of a number of orbital interactions in the system, including classic anomeric effect $n_X \rightarrow \sigma^*(C–H_{ax})$ and the hyperconjugation $\sigma(C–X) \rightarrow \sigma^*(C–H_{eq})$ for the α-C–H bonds, and the homoanomeric Plough effect $(n_X)_{ax} \rightarrow \sigma^*(C–H_{eq})$, W effect $(n_X)_{eq} \rightarrow \sigma^*(C–H_{eq})$, and $\sigma(C–H_{eq}) \rightarrow \sigma^*(C–X)$ for the β-C–H bonds, as well as the $\sigma(C–H_{ax}) \rightarrow \sigma^*(C–H_{ax})$ stereoelectronic interaction between the vicinal antiperiplanar C–H bonds. The relative contribution of these effects is strongly dependent on the nature of X.

Recently we have found that $^1J_{CH_{ax}}$ are larger than $^1J_{CH_{eq}}$ in the 3(5)-position of the ring for some 4-silathiane *S*-oxides. This was considered as the *reverse* Perlin effect in its original definition and rationalized in terms of the buttressing effect of the axial sulfinyl group on the 3(5)-C–$H_{ax}$ bonds.[23] However, this falls into Wolfe's modified definition[13,18a] of the *normal* Perlin effect (the longer C–H bond is usually associated with the lower one-bond C–H coupling constant) since the buttressing effect results in both increasing the $^1J_{CH_{ax}}$ values and shortening the 3(5)-C–$H_{ax}$ bonds.[23] Very recently we have found for 1-(methylsulfonyl)-3,5-bis(trifluoromethylsulfonyl)-1,3,5-triazinane (**2**) another example of the reverse Perlin effect,[11] which according to Alabugin[18a] should be considered as a *genuine* reverse Perlin effect since *all* C–$H_{ax}$ bonds in compound **2** are by 0.007–0.011 Å (at the B3LYP/6-311+G(d,p) level of theory) longer than the corresponding C–$H_{eq}$ bonds and still both the experiment and calculations gave $J_{CH_{ax}} > J_{CH_{eq}}$. This rationalization was based on the assumption that *syn*-periplanar $\sigma(C–H_{eq}) \rightarrow \sigma^*(N–S)$ stereoelectronic interactions should weaken the vicinal C–$H_{eq}$ bonds and decrease $J_{CH_{eq}}$. The same could be true for both rotamers of compound **1** and for 4-$CH_2$ in compound **3**. With this, the classic anomeric effect $n(N) \rightarrow \sigma^*(C–H_{ax})$ may still cause some elongation of the C–$H_{ax}$ bonds as is the case for molecules **1**–**3** in which all C–$H_{ax}$ bonds are by ~0.01 Å longer than the corresponding C–$H_{eq}$ bonds. The situation of the reverse Perlin effect when the larger value of $J_{CH_{ax}}$ is associated with the longer C–H bond was successfully simulated theoretically on a model compound.[11]

## 2.4. NBO analysis

The aforementioned attempts to correlate the observed Perlin effect with specific single stereoelectronic interactions or their combinations[11,13,15,18] prompted us to perform full NBO analysis in order to estimate the relative contribution of such interactions for the systems under investigation. The NBO analysis,[24] as implemented in the Gaussian 03 package,[25] was performed for the conformers of molecules **1**–**3** and, for comparison, for tetrahydropyran which shows the normal Perlin effect for the α-$CH_2$ group. The results

**Table 5**. Total second order perturbation energies (kcal/mol) for major orbital interactions of the donor σ(C–H) and acceptor σ*(C–H) orbitals in molecules **1**–**3** and in tetrahydropyran

| Molecule | Bond | σ(C–H) → all orbitals | All orbitals → σ*(C–H) |
|---|---|---|---|
| **1a** | 2-$CH_{ax}$ | 4.72 | 9.71 |
| | 2-$CH_{eq}$ | 7.85 | 3.53 |
| | 4-$CH_{ax}$ | 2.54 | 11.56 |
| | 4-$CH_{eq}$ | 7.92 | 3.26 |
| **1b** | $CH_{ax}$ | 4.49 | 10.02 |
| | $CH_{eq}$ | 8.02 | 1.60 |
| **2a** | 2-$CH_{ax}$ | 6.12 | 8.93 |
| | 2-$CH_{eq}$ | 7.81 | 3.75 |
| | 4-$CH_{ax}$ | 6.81 | 8.17 |
| | 4-$CH_{eq}$ | 7.70 | 3.62 |
| **3a** | 2-$CH_{ax}$ | 3.62 | 10.42 |
| | 2-$CH_{eq}$ | 7.91 | 5.01 |
| | 4-$CH_{ax}$ | 5.77 | 9.17 |
| | 4-$CH_{eq}$ | 7.15 | 3.73 |
| | 6-$CH_{ax}$ | 2.66 | 10.35 |
| | 6-$CH_{eq}$ | 7.03 | 5.02 |
| **3b** | 2-$CH_{ax}$ | 3.49 | 10.32 |
| | 2-$CH_{eq}$ | 7.67 | 5.12 |
| | 4-$CH_{ax}$ | 6.40 | 8.70 |
| | 4-$CH_{eq}$ | 7.22 | 3.76 |
| **THP** | 2-$CH_{ax}$ | 5.16 | 6.94 |
| | 2-$CH_{eq}$ | 5.97 | 3.49 |

are presented in Tables SI-1–SI-5 in Supplementary Data. The results definitely showed that the previously suggested effect of σ(C–$H_{eq}$) → σ*(N–S) interaction[11] in molecules **1**–**3** is less than 0.5 kcal/mol (the threshold for printing by default). Instead, the strongest interactions of the σ(C–$H_{eq}$) orbitals are those with the vicinal σ*(N–C) orbitals (7–8 kcal/mol) and they exceed the donor stereoelectronic interactions of the σ(C–$H_{ax}$) orbitals (2.5–6.8 kcal/mol). On the contrary, the acceptor stereoelectronic interactions of the σ*(C–$H_{eq}$) orbitals (1.6–3.8 kcal/mol) are notably less than the acceptor interactions of the σ*(C–$H_{ax}$) orbitals with the nitrogen lone pairs (8.2–11.5 kcal/mol).

Table 5 summarizes the total second order perturbation energies for major orbital interactions of the σ(C–H) and σ*(C–H) orbitals in the conformers of molecules **1**–**3** and in tetrahydropyran. The higher donor ability of the σ(C–$H_{eq}$) versus σ(C–$H_{ax}$) orbitals and the higher acceptor ability of the σ*(C–$H_{ax}$) versus σ*(C–$H_{eq}$) orbitals is obeyed for all pairs of the C–H bonds in Table 5, regardless of whether they show the normal (2,6-CH in **3**; 2-CH in THP) or reverse (all other) Perlin effect.

Thus, a discouraging conclusion is that the NBO analysis cannot account for the origin of the observed reverse Perlin effect. Probably, it is not only hyperconjugation but also a combination of several sources or polar influences, like those suggested in Refs. 20,21, that determine the resultant value of the $^1J_{CH}$ coupling constant.

## 3. Conclusion

Two dynamic processes, ring inversion and rotation about the N–S bond in 3,5-bis(trifluoromethylsulfonyl)-1,3,5-oxadiazinane **3**, were found and investigated by multinuclear dynamic NMR in conjunction with a theoretical study. These processes lead to the existence of two conformers with different orientation of the $CF_3SO_2$ group with respect to the heterocycle ring, both being observed experimentally. A large reverse Perlin effect ($J_{CH_{ax}} > J_{CH_{eq}}$) was found experimentally and proved theoretically for 1,3,5-tris(trifluoromethylsulfonyl)-1,3,5-triazinane, 1-(methylsulfonyl)-3,5-bis(trifluoromethylsulfonyl)-1,3,5-triazinane, and 3,5-bis(trifluoromethylsulfonyl)-1,3,5-oxadiazinane. Specific stereoelectronic orbital interactions, as followed from a parallel NBO analysis, do not account for the origin of the observed reverse Perlin effect as questioned generally very recently.[20,21]

## 4. Experimental

### 4.1. General remarks

Synthesis and physico-chemical characteristics of compounds **1**–**3** are described in our previous work.[8,10,11]

### 4.2. NMR measurements

Dynamic $^1H$, $^{13}C$, $^{15}N$, $^{19}F$ NMR spectra were recorded on a Bruker DPX 400 spectrometer at working frequencies 400 ($^1H$), 100 ($^{13}C$), 40 ($^{15}N$), and 376 ($^{19}F$) MHz; $^1H$ and $^{13}C$ NMR chemical shifts are reported in parts per million downfield to TMS and $^{19}F$ NMR in parts per million downfield to $CFCl_3$. $^{15}N$ NMR chemical shifts were obtained from 2D{$^1H$–$^{15}N$} spectra recorded by the use of a gradient probe working in the *hmbcgp* mode optimized to the long-range coupling constant $J_{NH}$ of 9 Hz, and are reported in parts per million downfield to $CH_3NO_2$. Temperature was varied by the use of a BVT 3000 variable temperature unit, temperature stability ±0.2°.

### 4.3. X-ray analysis

X-ray analysis of compound **3b** (Fig. 7) was performed on an Imaging Plate Diffraction System IPDS-2 (Stoe) at 210 K using the graphite monochromated Mo K$\alpha$ radiation. The structure (CCDC reference number 658418) was solved by direct method[26] and refined using the full matrix least squares method with SHELXL97.[27]

### 4.4. Theoretical calculations

All calculations were performed using the Gaussian 03 suite of programs.[27] Energy calculation with full optimization of all variables as well as calculation of vibrational frequencies was performed at the B3LYP/6-311+G(d,p) level of theory with the basis set augmented with polarization functions on heavy atoms. NMR computations of absolute shieldings and spin–spin coupling constants were performed using the GIAO method[28,29] at the same level of theory B3LYP/6-311+G(d,p). The $^1H$ and $^{19}F$ chemical shifts were calculated using the corresponding absolute shieldings calculated for $Me_4Si$ and $CFCl_3$ at the same level of theory.

## Acknowledgements

The financial support of this work by the Russian Foundation for Basic Research (Grant No. 07-03-00425) and Deutsche

Forschungsgemeinschaft (Grant RFBR-DFG No. 07-03-91559) is acknowledged.

## Supplementary data

Supplementary data include the second order perturbation energies (kcal/mol) for orbital interactions of the α-C–H bonds in tetrahydropyran from NBO computations at the B3LYP/6-311+G(d,p) level; 2D{$^1$H–$^{15}$N} spectrum of compound **1**; $^{13}$C NMR spectrum of **3** in $CD_3OD$ at 293 K; 2 D NOESY spectrum of **3** in acetone-$d_6$ at 193 K; cif file and ORTEP plot as well as further details of the crystal structure analysis for molecule **3b**. This material is available free of charge in the online version of the paper. Supplementary data associated with this article can be found in the online version, at doi:10.1016/j.tet.2007.09.041.

## References and notes

1. (a) *Conformational Behavior of Six-membered Rings. Analysis, Dynamics, and Stereoelectronic Effects*; Juaristi, E., Ed.; VCH: New York, NY, 1995; (b) Kleinpeter, E. *Adv. Heterocycl. Chem.* **2004**, *86*, 41–127; (c) Juaristi, E.; Ordoñez, M. Conformational Preference of the Sulfinyl Group in Six-membered Heterocycles. *Organic Sulfur Chemistry*; Page, P., Ed.; Academic: London, 1998; Vol. 2, Chapter 3, pp 64–95.
2. (a) Roux, M. V.; Jimenez, P.; Davalos, J. Z.; Notario, R.; Juaristi, E. *J. Org. Chem.* **2001**, *66*, 5343–5351; (b) Alabugin, I. V.; Manoharan, M. *J. Org. Chem.* **2004**, *69*, 9011–9024; (c) Freeman, F.; Derek, E. *J. Comput. Chem.* **2003**, *24*, 909–919; (d) Wiberg, K. B.; Hinz, W.; Jarret, R. M.; Aubrecht, K. B. *J. Org. Chem.* **2005**, *70*, 8381–8384.
3. (a) Kleinpeter, E.; Taddei, F.; Wacker, P. *Chem.—Eur. J.* **2003**, *9*, 1360–1368; (b) Kleinpeter, E.; Koch, A.; Pihlaja, K. *Tetrahedron* **2005**, *61*, 7349–7358; (c) Freeman, F.; Cha, C.; Fang, C.; Huang, F. C.; Hwang, J. H.; Louie, P. L.; Shainyan, B. A. *J. Phys. Org. Chem.* **2005**, *18*, 35–48; (d) Freeman, F.; Asgari, N.; Entezam, B.; Gomarooni, F.; Mac, J.; Nguyen, M. H.; Nguyen, N. N. T.; Nguyen, T. P.; Pham, N. B.; Sultana, P.; Welch, T. S.; Shainyan, B. A. *Int. J. Quantum Chem.* **2005**, *101*, 40–54; (e) Freeman, F.; Entezam, B.; Gomarooni, F.; Welch, T. S.; Shainyan, B. A. *J. Organomet. Chem.* **2005**, *690*, 4103–4113; (f) Freeman, F.; Shainyan, B. A. *Int. J. Quantum Chem.* **2005**, *105*, 313–324; (g) Shainyan, B. A. *Int. J. Quantum Chem.* **2007**, *107*, 189–199.
4. Shainyan, B. A.; Kirpichenko, S. V. *Russ. J. Gen. Chem. (Engl. Transl.)* **2003**, *73*, 1709–1714.
5. Jewett, J. G.; Breeyear, J. J.; Brown, J. H.; Bushweller, C. H. *J. Am. Chem. Soc.* **2000**, *122*, 308–323.
6. Anderson, J. E.; Casarini, D.; Ijeh, A. I.; Lunazzi, L.; Tocher, D. A. *J. Am. Chem. Soc.* **1995**, *117*, 3054–3056.
7. dos Santos, F. P.; Tormena, C. F. *J. Mol. Struct.* **2006**, *763*, 145–148.
8. Mescheryakov, V. I.; Albanov, A. I.; Shainyan, B. A. *Russ. J. Org. Chem. (Engl. Transl.)* **2005**, *41*, 1381–1386.
9. Mescheryakov, V. I.; Danilevich, Yu. S.; Moskalik, M. Yu.; Stetsjura, N. Yu.; Zavodnik, V. E.; Bel'skii, V. K.; Shainyan, B. A. *Russ. J. Org. Chem. (Engl. Transl.)* **2007**, *43*, 793–800.
10. Shainyan, B. A.; Mescheryakov, V. I.; Albanov, A. I.; Sigalov, M. V. *Tetrahedron Lett.* **2005**, *46*, 6199–6201.
11. Shainyan, B. A.; Ushakov, I. A.; Koch, A.; Kleinpeter, E. *J. Org. Chem.* **2006**, *71*, 7638–7642.
12. Perlin, A. S.; Casu, B. *Tetrahedron Lett.* **1969**, *10*, 2921–2924.
13. (a) Wolfe, S.; Pinto, B. M.; Varma, V.; Leung, R. Y. N. *Can. J. Chem.* **1990**, *68*, 1051–1062; (b) Wolfe, S.; Kim, C.-K. *Can. J. Chem.* **1991**, *69*, 1408–1412.
14. Bailey, W. F.; Rivera, A. D.; Rossi, K. *Tetrahedron Lett.* **1988**, *29*, 5621–5624.
15. (a) Juaristi, E.; Cuevas, G. *Tetrahedron* **1992**, *48*, 5019–5087; (b) Juaristi, E.; Cuevas, G. *Tetrahedron Lett.* **1992**, *33*, 1847–1850; (c) Juaristi, E.; Cuevas, G.; Flores-Vela, A. *Tetrahedron Lett.* **1992**, *33*, 6927–6930; (d) Juaristi, E.; Cuevas, G.; Vela, A. *J. Am. Chem. Soc.* **1994**, *116*, 5796–5804; (e) Cuevas, G.; Juaristi, E.; Vela, A. *J. Mol. Struct.* **1997**, *418*, 231–241; (f) Cuevas, G.; Juaristi, E.; Vela, A. *J. Phys. Chem. A* **1999**, *103*, 932–937; (g) Cuevas, G.; Juaristi, E. *J. Am. Chem. Soc.* **2002**, *124*, 13088–13096; (h) Juaristi, E.; Rosquete-Pina, G. A.; Vásquez-Hernández, M.; Mota, A. J. *Pure Appl. Chem.* **2003**, *75*, 589–599.
16. (a) Anderson, J. E.; Bloodworth, A. J.; Cai, J. Q.; Davies, A. G.; Schiesser, C. H. *J. Chem. Soc., Perkin Trans. 2* **1993**, 601–602; (b) Cai, J. Q.; Davies, A. G.; Schiesser, C. H. *J. Chem. Soc., Perkin Trans. 2* **1994**, 1151–1156; (c) Anderson, J. E.; Bloodworth, A. J.; Cai, J. Q.; Davies, A. G.; Tallant, N. A. *J. Chem. Soc., Chem. Commun.* **1992**, 1689–1690; (d) Anderson, J. E.; Cai, J. Q.; Davies, A. G. *J. Chem. Soc., Perkin Trans. 2* **1997**, 2633–2638.
17. Randell, K. D.; Johnston, B. D.; Green, D. F.; Pinto, B. M. *J. Org. Chem.* **2000**, *65*, 220–226.
18. (a) Alabugin, I. V. *J. Org. Chem.* **2000**, *65*, 3910–3919; (b) Alabugin, I. V.; Manoharan, M.; Zeidan, T. A. *J. Am. Chem. Soc.* **2003**, *125*, 14014–14031.
19. Freeman, F.; Cha, C. *J. Phys. Org. Chem.* **2004**, *17*, 32–41.
20. Cuevas, G.; Martínez-Mayorga, K.; Fernández-Alonso, M. C.; Jiménez-Barbero, J.; Perrin, C. L.; Juaristi, E.; López-Mora, N. *Angew. Chem., Int. Ed.* **2005**, *44*, 2360–2364.
21. Perrin, C. L.; Erdélyi, M. *J. Am. Chem. Soc.* **2005**, *127*, 6168–6169.
22. Contreras, R. H.; Esteban, A. L.; Diez, E.; Della, E. W.; Lochert, I. J.; dos Santos, F. P.; Tormena, C. F. *J. Phys. Chem. A* **2006**, *110*, 4266–4275.
23. Shainyan, B. A.; Ushakov, I. A.; Suslova, E. N. *J. Sulfur Chem.* **2006**, *27*, 3–13.
24. (a) Weinhold, F.; Landis, C. R. *Valency and Bonding: A Natural Bond Orbital Donor–Acceptor Perspective*; Cambridge University Press: Cambridge, 2005; (b) Glendening, E. D.; Reed, A. E.; Carpenter, J. E.; Weinhold, F. *NBO Version 3.1*; Gaussian: Pittsburgh, PA, CT, 2003.
25. Frisch, M. J.; Trucks, G. W.; Schlegel, H. B.; Scuseria, G. E.; Robb, M. A.; Cheeseman, J. R.; Montgomery, J. A., Jr.; Vreven, T.; Kudin, K. N.; Burant, J. C.; Millam, J. M.; Iyengar, S. S.; Tomasi, J.; Barone, V.; Mennucci, B.; Cossi, M.; Scalmani, G.; Rega, N.; Petersson, G. A.; Nakatsuji, H.; Hada, M.; Ehara, M.; Toyota, K.; Fukuda, R.; Hasegawa, J.; Ishida, M.; Nakajima, T.; Honda, Y.; Kitao, O.; Nakai, H.; Klene, M.; Li, X.; Knox, J. E.; Hratchian, H. P.; Cross, J. B.; Bakken, V.; Adamo, C.; Jaramillo, J.; Gomperts, R.; Stratmann, R. E.; Yazyev, O.; Austin, A. J.; Cammi, R.; Pomelli, C.; Ochterski, J. W.; Ayala, P. Y.; Morokuma, K.; Voth, G. A.; Salvador, P.; Dannenberg, J. J.; Zakrzewski, V. G.; Dapprich, S.; Daniels, A. D.; Strain, M. C.; Farkas, O.; Malick, D. K.; Rabuck, A. D.; Raghavachari, K.; Foresman, J. B.; Ortiz, J. V.; Cui, Q.; Baboul, A. G.;

Clifford, S.; Cioslowski, J.; Stefanov, B. B.; Liu, G.; Liashenko, A.; Piskorz, P.; Komaromi, I.; Martin, R. L.; Fox, D. J.; Keith, T.; Al-Laham, M. A.; Peng, C. Y.; Nanayakkara, A.; Challacombe, M.; Gill, P. M. W.; Johnson, B.; Chen, W.; Wong, M. W.; Gonzalez, C.; Pople, J. A. *Gaussian 03, Revision B.03*; Gaussian: Pittsburgh, PA, CT, 2003.

26. Sheldrick, G. M. *SHELXS-97. Program for Crystal Structure Solution*; Göttingen University: Göttingen, Germany, 1997.
27. Sheldrick, G. M. *SHELXL-97. Program for Crystal Structure Refinement*; Göttingen University: Göttingen, Germany, 1997.
28. Ditchfield, R. *J. Chem. Phys.* **1972**, *56*, 5688–5691.
29. Wolinski, K.; Hinton, J. F.; Pulay, P. *J. Am. Chem. Soc.* **1990**, *112*, 8251–8260.